Critical Role of Monoclinic Polarization Rotation in High-Performance Perovskite Piezoelectric Materials

Hui Liu, Jun Chen, Longlong Fan, Yang Ren, Zhao Pan, K. V. Lalitha, Jürgen Rödel, and Xianran Xing

Phys. Rev. Lett. **119**, 017601 — Published 7 July 2017

DOI: 10.1103/PhysRevLett.119.017601

Critical Role of Monoclinic Polarization Rotation in High-performance Perovskite Piezoelectric Materials

Hui Liu,[1] Jun Chen,[1,*] Longlong Fan,[1] Yang Ren,[2] Zhao Pan,[1] Lalitha K. V.,[3] Jürgen Rödel,[3] and Xianran Xing[1]

[1]Department of Physical Chemistry, University of Science and Technology Beijing, Beijing 100083, China

[2]X-Ray Science Division, Advanced Photon Source, Argonne National Laboratory, Argonne, Illinois 60439, USA

[3]Institute of Materials Science, Technische Universität Darmstadt, Darmstadt 64287, Germany

*Corresponding author. junchen@ustb.edu.cn

Abstract

High-performance piezoelectric materials constantly attract the interest both for technological applications and fundamental research. The understanding of the origin for the high-performance piezoelectric property remains a challenge mainly due to the lack of direct experimental evidence. We have performed in-situ high-energy X-ray diffraction combined with 2D geometry scattering technology to reveal the underlying mechanism for the perovskite-type lead-based high-performance piezoelectric materials. The direct structural evidence has revealed that the electric-field-driven continuous polarization rotation within the monoclinic plane plays a critical role to achieve the giant piezoelectric response. An intrinsic relationship between crystal structure and piezoelectric performance in perovskite ferroelectrics has been established: A strong tendency of electric-field-driven polarization rotation generates peak piezoelectric performance and vice versa. Furthermore, the monoclinic M_A structure is the key feature to superior piezoelectric properties as compared to other structures such as monoclinic M_B, rhombohedral and tetragonal. High piezoelectric response originates from intrinsic lattice strain, but little from extrinsic domain switching. The present results will facilitate designing high-performance perovskite piezoelectric materials by enhancing the intrinsic lattice contribution with easy and continuous polarization rotation.

Piezoelectric materials, which convert mechanical energy into electrical energy and vice versa, are crucial in modern applications for electromechanical devices. Most of the high-performance piezoelectric materials have perovskite structure and form a morphotropic phase boundary (MPB) with tetragonal $PbTiO_3$, such as $PbMg_{1/3}Nb_{2/3}O_3$-$PbTiO_3$, $Pb(Zr,Ti)O_3$ and their ternary systems [1,2]. Recently, there has been considerable interest in developing lead-free piezoelectric materials [3-5]. However, no lead-free alternatives have been found that can completely replace the lead-based materials until now. To overcome this situation, it is essential to understand the origin of high-performance of piezoelectricity.

Several theories have been put forward to achieve this goal. Firstly, the coexistence of tetragonal (T) and rhombohedral (R) phases near the MPB region has been proposed to enhance the piezoelectric property by enabling more switchable polarization directions or the additional interphase transformation [1,6-8]. In 1999, Noheda *et al* discovered the important low symmetry monoclinic (M) structure in $Pb(Zr_{0.52}Ti_{0.48})O_3$ [9], which has also been corroborated in other systems [10-13]. High piezoelectric response was assigned to the polarization rotation mechanism [2,14,15]. The polarization rotation path via an intermediate monoclinic among tetragonal, rhombohedral, orthorhombic phases has been intensively studied for various lead-based piezoelectrics [11-13,16-19]. The monoclinic phase is believed to be the bridge of polarization between morphotropic phases and provides for a flexible polarization rotation [11,12,14,15]. The high-performance piezoelectricity is mainly attributed to the large shear piezoelectric response [13,20,21] which is considered to be directly linked to polarization rotation [22]. Especially, the thermodynamic

analysis has elucidated the polarization rotation as a consequence of the flattening of the free energy profile near the MPB [22,23]. In addition, mesoscopic models have also been proposed, such as the nanodomain and adaptive ferroelectric phase state [24,25].

However, no direct structural proof has been provided for the continuous polarization rotation and its intrinsic correlation to high-performance piezoelectricity. Recently, we have employed the method of in-situ high-energy synchrotron X-ray diffraction (SXRD) combined with 2D scattering geometry, which affords the possibility to simultaneously extract the information of crystal structure, domain switching, and lattice strain of piezoelectric materials [18].

In this Letter, we have studied several lead-based piezoceramic systems with high or moderate performance by in-situ high-energy SXRD. Phase structure, domain switching and in particular, the process of polarization rotation are analyzed as function of electric field. The present study reveals the unique polarization rotation within the $(110)_{PC}$ plane of the monoclinic phase, and delivers direct structural evidence for the giant piezoelectric response. The summary of the intrinsic structure-property correlation will be helpful for designing new high-performance piezoelectric materials in the future.

Several lead-based piezoceramic systems have been fabricated by solid-state reaction method, which include both high and moderate performance. The high-performance systems are $0.675Pb(Mg_{1/3}Nb_{2/3})O_3$-$0.325PbTiO_3$ (PMN-PT, d_{33} = 670 pC/N), $0.41Pb(Ni_{1/3}Nb_{2/3})O_3$-$0.23PbZrO_3$-$0.36PbTiO_3$ (PNN-PZT, d_{33} = 650 pC/N), $0.128Pb(Mg_{1/3}Nb_{2/3})O_3$-$0.336Pb(Ni_{1/3}Nb_{2/3})O_3$-$0.536PbTiO_3$ (PMN-PNN-PT,

d_{33} = 600 pC/N). A moderate-performance system was included with $0.33Pb(Ni_{1/3}Nb_{2/3})O_3$-$0.67PbTiO_3$ (PNN-PT, d_{33} = 400 pC/N). By using the present method of in-situ high-energy SXRD technology combined with appropriate 2D scattering geometry (see Fig. S1(a), of the Supplemental Material [26]), the diffraction patterns at the 45° sectors contain negligible effects of preferred orientation, which allows extracting the important piezoelectric-related structure information, such as the polarization rotation behavior. This strategy to minimize the effect of preferred orientation is analogous to the important method reported by Hinterstein *et al*. [16,36]. The in-situ diffraction data were collected during the unloading procedure from an electric field near the coercive field (E_C) to zero electric field (E = 0 kV/mm). More experimental details are provided in the Supplemental Material [26].

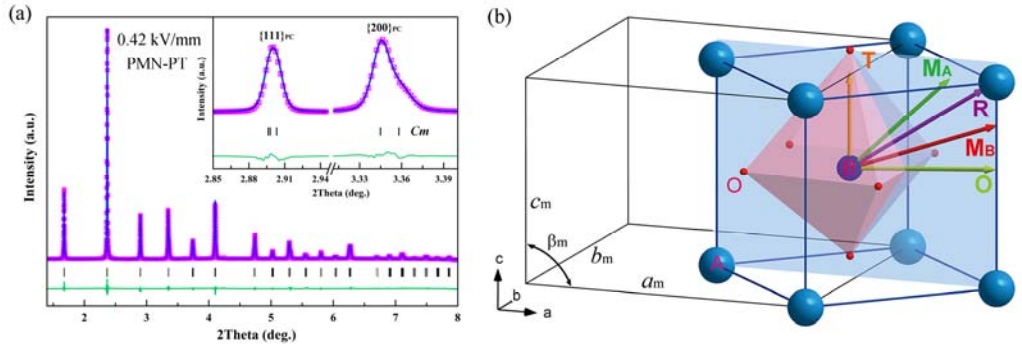

FIG. 1. (a) Full-profile Rietveld refinement of the monoclinic phase of PMN-PT at the 45° sector under 0.42 kV/mm. The observed data (pink points), the calculated profile (blue line), and the difference between the observed and calculated patterns (bottom green line) are depicted. The thick marks indicate the Bragg peak positions of the *Cm* phase. The inset provides the enlarged profiles of $\{111\}_{PC}$ and $\{200\}_{PC}$. (b) Schematic

illustration for the polarization vectors in the $(110)_{PC}$ plane of monoclinic (*Cm*) and other phases. M_A, M_B, T, R and O specifies monoclinic M_A, monoclinic M_B, tetragonal, rhombohedral, and orthorhombic structures, respectively.

It is intriguing to note that after electric field poling a single monoclinic phase has been achieved for all four piezoceramic systems of PMN-PT, PNN-PZT, PMN-PNN-PT and PNN-PT. Here, we focus on determination of the electric-field induced monoclinic phase. Firstly, according to the high angle $\{400\}_{PC}$ profile with the character of two distinct peaks (Fig. S4 of Ref. [26]), and the asymmetry of the $\{222\}_{PC}$ profile as function of azimuthal angle (Fig. S5 of Ref. [26]), the tetragonal, rhombohedral and orthorhombic phase could be tentatively excluded. The results of Rietveld refinement show that the monoclinic (*Cm*) phase yields the best agreement. For instance, for PMN-PT ceramic at 0.42 kV/mm [Fig. 1(a)], the agreement factor is R_{wp} = 3.26% for the *Cm* model, while worse refinements were achieved in other models such as *R*3*m*, *P*4*mm*, *P*4*mm*+*R*3*m*, *Pm*, and *Bmm*2 with higher R_{wp} values of 4.14%, 3.46%, 3.43%, 3.46% and 3.47%, respectively (Table S1 of Ref. [26]). Accordingly, it can be confirmed that a single monoclinic phase (*Cm*) exists for the present studied piezoelectric systems. Extensive details on structure analysis are provided in the Supplemental Material [26].

Even though all these piezoceramic systems exhibit the same monoclinic structure (*Cm*), it is interesting to observe that there is a definitive difference in polarization behavior. The high-performance systems of poled PMN-PT, PNN-PZT and PMN-PNN-PT exhibit M_A polarization behavior at 0 kV/mm, while the

moderate-performance PNN-PT displays M_B behavior [Fig. 1(b)]. A common feature of M_A and M_B is that the polarization is constrained within the $(110)_{PC}$ plane, but the difference is that the monoclinic M_A has the polarization lying between $[001]_{PC}$ and $[111]_{PC}$ directions which acts as a bridge between T and R phase, while the polarization of the M_B phase lies between the $[110]_{PC}$ and $[111]_{PC}$ directions which acts as a bridge between O and R phases [19]. Here, we define the angle between the polarization vector and the $[001]_{PC}$ direction as θ (Fig. S9 of Ref. [26]). It is easy to see that when θ around is 0~54.7°, it is in the M_A region, while θ around 54.7°~90° belongs to the M_B region.

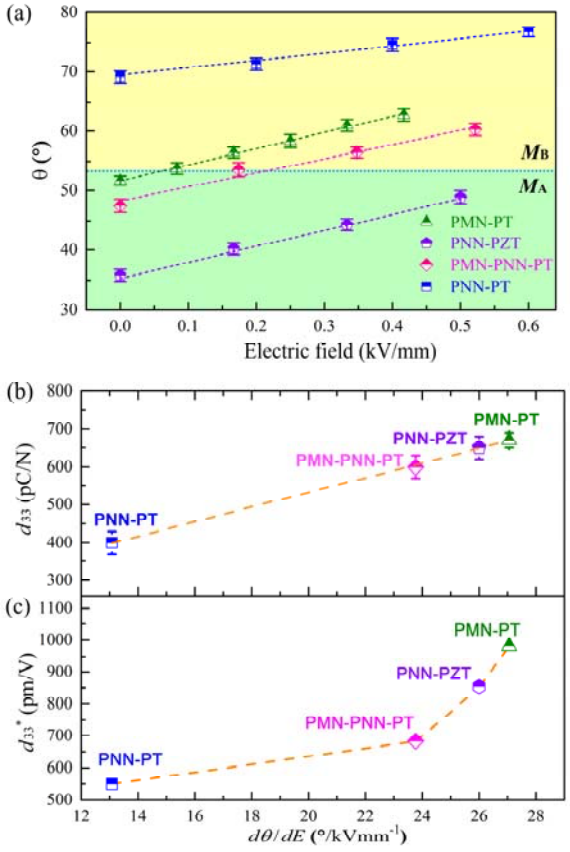

FIG. 2. (a) The angle of polarization vector as function of electric field (θ *vs.* E). The

boundary of M_A and M_B phases is indicated by the dashed line. (b) The macroscopic measured piezoelectric coefficient d_{33}, and (c) the calculated piezoelectric coefficient d_{33}^* from intrinsic lattice strain as a function of $d\theta/dE$.

After performing the full-profile Rietveld refinements for four monoclinic piezoelectric systems at various electric fields, the electric field-driven polarization properties can be obtained. The present study reveals critical evidence of the electric field-driven continuous polarization rotation, θ *vs.* E [Fig. 2(a)]. At 0 kV/mm, all the three piezoceramic systems of PMN-PT, PNN-PZT, PMN-PNN-PT with relatively higher d_{33} exhibit the M_A phase, but PNN-PT with relatively lower d_{33} features the M_B phase. Upon increasing electric field, electric-field-driven continuous polarization rotation sets in, which has never been observed before. For the PNN-PZT and PNN-PT, they remain in the same monoclinic region. However, there is an electric-field-driven M_A-to-M_B polarization transformation for the PMN-PT and PMN-PNN-PT. Note that in the $0.65Pb(Mg_{1/3}Nb_{2/3})O_3$-$0.35PbTiO_3$ single crystals, the monoclinic M_A structure has been observed under applied weak electric field [10].

The value of polarization can be estimated by considering a purely ionic state. The magnitude of polarization in four piezoelectric systems almost maintains unchanged in the studied electric field range (Fig. S10 of Ref. [26]), which indicates that electric field drives the rotation but not the magnitude change of polarization vectors.

As displayed in Fig. 2(a), there is a linear relationship for θ *vs.* E. Here, the slope is defined as $d\theta/dE$. A large value of $d\theta/dE$ defines extensive electric-field-driven polarization rotation, while a small one describes limited polarization rotation. There

is significant difference in the $d\theta/dE$ for the four piezoelectric systems, in which PMN-PT (27.1 °/(kVmm^{-1})), PNN-PZT (26 °/(kVmm^{-1})), and PMN-PNN-PT (23.8 °/(kVmm^{-1})) exhibit larger values but PNN-PT (13.1 °/(kVmm^{-1})) a smaller one. We can find a direct correlation between the rate of polarization rotation $d\theta/dE$ and the macroscopic measured piezoelectric coefficient d_{33} [Fig. 2(b)]. The higher rate of polarization rotation conforms to a high piezoelectric coefficient d_{33}. A large value of $d\theta/dE$ empowers a small electric field to drive a large change of polarization vector angle. This critical role of polarization rotation can also be supported by the phenomenon that the electric field necessary for polarization rotation decreases significantly when approaching the critical point where the piezoelectric performance is maximum such as in the PMN-PT single crystals [11]. This is in accordance with Landau-Ginsburg-Devonshire (LGD) phenomenological theory as facilitated polarization rotation manifests large dielectric susceptibility, and therefore gives rise to large piezoelectric response [23].

Piezoelectric response is generally contributed from the intrinsic lattice strain and extrinsic domain switching effects. Since the present four piezoelectric systems exhibit a single monoclinic structure, the extrinsic domain switching and the intrinsic lattice strain contributions can be extracted from the $\{002\}_{PC}$ profile at the 0° sector, which was fitted by two peaks using Pseudo-Voigt function [18]. The changes of integrated intensities of the reflections can be correlated to the domain switching (η_{norm}). η_{norm} indicates the normalized relative volume fraction of switched domains, which is suitable for comparison among different symmetries. The position shift of the reflections can be utilized for evaluating the lattice strain (ε) [18,37-41]. The

electric field dependence of η_{norm} is plotted in Fig. S11(a) of Ref. [26]. Firstly, it is interesting to find that the monoclinic phase exhibits a very large domain rearrangement fraction by electric poling. The value of η_{norm} is above 70% for the four piezoelectric systems after the release of electric field, which is much higher than that of T and R phases [37, 38]. A large value of η_{norm} was also observed in the monoclinic $PbZr_{0.535}Ti_{0.465}O_3$ ceramic [18]. It strongly supports the notion that the non-180° domains of the monoclinic phase are much easier aligned to electric field direction as compared to the tetragonal and rhombohedral ones [42]. Secondly, monoclinic phase exhibits negligible domain switching after electric poling. To quantitatively estimate the domain switching of monoclinic phase as function of electric field, the ratio of $\Delta\eta_{norm}/\Delta E$ was calculated. It is as small as 0.43%/(kVcm^{-1}), 0.67%/(kVcm^{-1}), 0.19%/(kVcm^{-1}), 1.15%/(kVcm^{-1}) for the monoclinic phase in the PMN-PT, PNN-PZT, PMN-PNN-PT, PNN-PT, respectively. This implies that the monoclinic phase exhibits a common behavior of negligible domain switching, when compared with those of T and R phases [18,39,40]. Thus, the piezoelectric response of the monoclinic phase must originate from the intrinsic contribution of lattice strain.

The electric field dependence of lattice strain is provided in Fig. S11(b) of Ref. [26]. The $(200)_{PC}$ strain reveals a linear relationship with electric field, in which the slope indicates the piezoelectric coefficient d_{33}^* of intrinsic lattice strain. PMN-PT, PNN-PZT, PMN-PNN-PT and PNN-PT exhibit 982 pm/V, 854 pm/V, 684 pm/V, and 564 pm/V, respectively. Similarly, d_{33}^* is also correlated with $d\theta/dE$ [Fig. 2(c)]. The present results lead to the conclusion that the monoclinic phase exhibits common piezoelectric properties of negligible domain switching and large lattice strain.

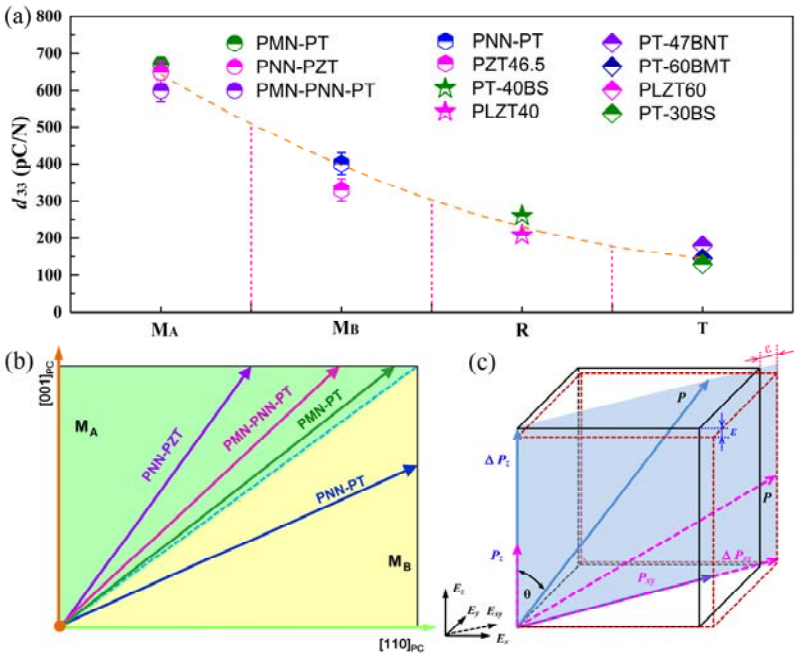

FIG. 3. (a) The relationship between the macroscopic measured d_{33} and phase structure. The other d_{33} values of PT-100xBS ((1-x)$PbTiO_3$-$x$$BiScO_3$)), PT-60BMT (0.4$PbTiO_3-0.6BiMg_{1/2}Ti_{1/2}O_3$), PT-47BNT (0.53$PbTiO_3-0.47BiNi_{1/2}Ti_{1/2}O_3$) and La doped $PbZr_{1-x}Ti_xO_3$ (PLZT100x) are adopted from the literature [39, 43-45]. (b) Schematic illustration of monoclinic polarization vectors at zero electric field in the $(110)_{PC}$ plane. The boundary between M_A and M_B is indicated by the dashed line. (c) Schematic illustration of the coupling between electric-field-driven-polarization rotation and intrinsic lattice strain.

As presented in Fig. 2 (b) and (c), the critical role of monoclinic polarization rotation for the high-performance of piezoelectrics has been corroborated. Here we emphasize the fundamental relationship between the piezoelectric property and crystal structure for lead-based perovskites [Fig. 3(a)]. Importantly, the M_A phase corresponds to the highest piezoelectric performance, while the other crystal

structures of M_B, R and T yield more or less inferior piezoelectric performance. The polarization vectors of monoclinic phase under zero electric field are highlighted as an example in Fig. 3(b). For the M_A structure, the polarization can rotate from the direction between $[001]_{PC}$ and $[111]_{PC}$, with a larger range of θ variation (54.7º). However, for the M_B structure the polarization rotates between $[111]_{PC}$ and $[110]_{PC}$ with a smaller range of θ variation (35.3º). The piezoelectric response is strongly coupled to polarization variation. The extension of the polarization component is connected to the intrinsic lattice strain when the polarization rotation is driven by the electric field [Fig. 3(c)]. The origin of the enhancement of piezoelectric activity has been widely demonstrated by the LGD thermodynamic theory calculation in the T, R, and O phase in the MPB region [14,23,46,47]. It is believed that the M_A structure would be more beneficial to polarization rotation than the M_B structure due to the flatter free energy profile [14]. The low contribution by the anisotropic free energy indicates enhanced susceptibility of the atomic displacements, resulting in giant piezoelectric performance [23,47]. Therefore, it is much easier to achieve higher performance of piezoelectrics in the M_A structure. Also in the previous first-principle calculation for the single crystal $BaTiO_3$ the piezoelectric responses of the M_A path is 5 times larger that of the M_B path [14].

Additionally, much inferior piezoelectric property of the T and R phases is due to fewer available polarization directions. There are only 8 for rhombohedral and 6 directions for tetragonal phase in comparison to the monoclinic phase (24 polarization directions). In the perovskite ferroelectrics, the crystallographic symmetry has a strong influence on ferroelectric domain switching [42]. Compared to the advantage

of the continuous rotation of polarization in the monoclinic phase, the polarization vector is fixed in one of the directions of $[001]_{PC}$ for the T phase and $[111]_{PC}$ for the R phase. The polarization of T and R phases is not allowed to smoothly rotate under the electric field. Thus much inferior piezoelectric property is generated.

The present understanding of the piezoelectric mechanism will be helpful for the design of high-performance perovskite piezoelectric materials in the future. It is pertinent to obtain the crystal structure which enables polarization rotation smoothly driven by electric field in order to obtain a piezoelectric with higher performance.

In summary, a single electric field-induced monoclinic phase has been identified in compositions of all four systems of PMN-PT, PNN-PZT, PMN-PNN-PT and PNN-PT. A visualized polarization rotation within the $(110)_{PC}$ plane of the monoclinic phase driven by electric field has been observed. In perovskite ferroelectrics, a direct correlation between structure and piezoelectric property has been established. Monoclinic M_A phase indicates a superior piezoelectric property and other structures such as M_B, R, T exhibit inferior property. The piezoelectric property depends critically on the sensitivity of polarization rotation to electric field. A strong tendency of electric-field-driven polarization rotation generates peak piezoelectric performance. It is mainly attributed to intrinsic lattice strain and little to extrinsic domain wall motion. The present results reveal that the sensitivity of polarization rotation plays a key role in the design of new high-performance piezoelectric materials in the future.

This work was supported by the National Natural Science Foundation of China (Grant Nos. 21322102, 91422301, 21231001, 21590793), National Program for Support of Top-notch Young Professionals, Program for Chang Jiang Young Scholars,

and the Fundamental Research Funds for the Central Universities, China (Grant No.FRF-TP-14-012C1). This research used resources of the Advanced Photon Source, a U.S. Department of Energy (DOE) Office of Science User Facility operated for the DOE Office of Science by Argonne National Laboratory under Contract No. DE-AC02-06CH11357.

[1] B. Jaffe, W. R. Cook, and H. Jaffe, London, *Piezoelectric Ceramics* (Academic Press, New York, 1971).

[2] S. E. Park, and T. R. Shrout, J. Appl. Phys. **82**, 1804 (1997).

[3] Y. Saito, H. Takao, T. Tani, T. Nonoyama, K. Takatori, T. Homma, and M. Nakamura, Nature **432**, 84 (2004).

[4] J. Rödel, W. Jo, K. T. Seifert, E. M. Anton, T. Granzow, and D. Damjanovic, J. Am. Ceram. Soc. **92,** 1153 (2009).

[5] X. Liu, and X. Tan, Adv. Mater. **28**, 574 (2016).

[6] M. Hinterstein, M. Hoelzel, J. Rouquette, J. Haines, J. Glaum, H. Kungl, and M. Hoffman, Acta Mater. **94**, 319 (2015).

[7] M. Hinterstein, L. A. Schmitt, M. Hoelzel, W. Jo, J. Rödel, H. J. Kleebe, and M. Hoffman, Appl. Phys. Lett. **106**, 222904 (2015).

[8] N. H. Khansur, M. Hinterstein, Z. Wang, C. Groh, W. Jo, and J. E. Daniels, Appl. Phys. Lett. **107**, 242902 (2015).

[9] B. Noheda, D. E. Cox, G. Shirane, J. A. Gonzalo, L. E. Cross, and S. E. Park, Appl. Phys. Lett. **74**, 2059 (1999).

[10] Z. G. Ye, B. Noheda, M. Dong, D. Cox, and G. Shirane, Phys. Rev. B **64**, 184114 (2001).

[11] Z. Kutnjak, J. Petzelt, and R. Blinc, Nature **441**, 956 (2006).

[12] M. Ahart, M. Somayazulu, R. E. Cohen, P. Ganesh, P. Dera, H. K. Mao, R. J. Hemley Y. Ren, and Z. Wu, Nature **451**, 545 (2008).

[13] B. Noheda, D. E. Cox, G. Shirane, S. E. Park, L. E. Cross, and Z. Zhong, Phys. Rev. Lett. **86**, 3891 (2001).

[14] H. Fu, and R. E. Cohen, Nature **403**, 281 (2000).

[15] L. Bellaiche, A. García, and D. Vanderbilt, Phys. Rev. B **64**, 060103 (2001).

[16] M. Hinterstein, J. Rouquette, J. Haines, P. Papet, M. Knapp, J. Glaum, and H. Fuess, Phys. Rev. Lett. **107**, 077602 (2011).

[17] N. Zhang, H. Yokota, A. M. Glazer, Z. Ren, D. A. Keen, D. S. Keeble, P. A. Thomas, and Z. G. Ye, Nat. Commun. **5**, 5231 (2014).

[18] L. L. Fan, J. Chen, Y. Ren, Z. Pan, L. X. Zhang, and X. R. Xing, Phys. Rev. Lett. **116**, 027601 (2016).

[19] D. Vanderbilt, and M. H. Cohen, Phys. Rev. B **63**, 094108 (2001).

[20] M. Davis, M. Budimir, D. Damjanovic, and N. Setter, J. Appl. Phys. **101**, 054112 (2007).

[21] R. Zhang, B. Jiang, and W. Cao, Appl. Phys. Lett. **82**, 3737 (2003).

[22] D. Damjanovic, IEEE Trans. Ultrasonics, Ferroelectrics, Frequency Control, **56**, 1574 (2009).

[23] D. Damjanovic, J. Am. Ceram. Soc. **88**, 2663 (2005).

[24] R. Theissmann, L. A. Schmitt, J. Kling, R. Schierholz, K. A. Schönau, H. Fuess, and M. J. Hoffmann, J. Appl. Phys. **102**, 024111 (2007).

[25] Y. M. Jin, Y. U. Wang, A. G. Khachaturyan, J. F. Li, and D. Viehland, Phys. Rev. Lett. **91**, 197601 (2003).

[26] See Supplemental Material at http://link.aps.org/supplemental/, for details of the experimental setup, data processing, determination of phase structure, and supporting figures and tables, which includes Refs. [27-35].

[27] J. Rodríguez-Carvajal, Physica B **192**, 55 (1993).

[28] A. K. Singh, D. Pandey, and O. Zaharko, Phys. Rev. B **68**, 172103 (2003).

[29] B. Noheda, D. E. Cox, G. Shirane, J. Gao and Z. G. Ye, Phys. Rev. B **66**, 054104 (2002).

[30] N. Zhang, H. Yokota, A. M. Glazer, and P. A. Thomas, Acta Crystallogr. B **67**, 386, (2011).

[31] J. Chen, L. L. Fan, Y. Ren, Z. Pan, J. X. Deng, R. B. Yu, and X. R. Xing, Phys. Rev. Lett. **110**, 115901 (2013).

[32] R. Haumont, A. Al-Barakaty, B. Dkhil, J. M. Kiat, L. Bellaiche, Phys. Rev. B **71** (2005) 104106.

[33] J. Carreaud, J. M.Kiat, B. Dkhil, M. Alguero, J. Ricote, R. Jimenez, J. Holc and M. Kosec. Appl. Phys. Lett. **89**, 252906 (2006).

[34] J. Lohmiller, R. Baumbusch, O. Kraft, and P. A. Gruber, Phys. Rev. Lett. **110**, 066101 (2013).

[35] J. E. Daniels, J. L. Jones, and T. R. Finlayson, J. Phys. D: Appl. Phys. **39**, 5294 (2006).

[36] M. Hinterstein, J. Rouquette, J. Haines, Ph. Papet, J. Glaum, M. Knapp, J. Eckert, and M. Hoffman, Phys. Rev. B **90**, 094113 (2014).

[37] K. V. Lalitha, C. M. Fancher, J. L. Jones, and R. Ranjan, Appl. Phys. Lett. **107**, 052901 (2015).

[38] M. C. Ehmke, N. H. Khansur, J. E. Daniels, J. E. Blendell, and K. J. Bowman, Acta Mater. **66**, 340 (2014).

[39] A. Pramanick, J. E. Daniels, and J. L. Jones, J. Am. Ceram. Soc. **92**, 2300 (2009).

[40] A. Pramanick, D. Damjanovic, J. E. Daniels, J. C. Nino, and J. L. Jones, J. Am. Ceram. Soc. **94**, 293 (2011).

[41] J. L. Jones, M. Hoffman, and K. J. Bowman, J. Appl. Phys. **98**, 024115 (2005).

[42] J. Y. Li, R. C. Rogan, E. Üstündag, and K. Bhattacharya, Nature Mater. **4**, 776 (2005).

[43] Lalitha K. V., A. N. Fitch, and R. Ranjan, Phys. Rev. B **87**, 064106 (2013).

[44] C. A. Randall, R. Eitel, B. Jones, T. R. Shrout, D. I. Woodward, and I. M. Reaney, J. Appl. Phys. **95**, 3633 (2004).

[45] S. M. Choi, C. J. Stringer, T. R. Shrout, and C. A. Randall, J. Appl. Phys. **98**, 34108 (2005).

[46] M. Acosta, N. Khakpash, T. Someya, N. Novak, W. Jo, H. Nagata, G. A. Rossetti, and J. Rödel, Phys. Rev. B, **91**, 104108 (2015).

[47] A. G. Khachaturyan, Philos. Mag. **90**, 37 (2010).